Egypt. J. Chem. **Vol. 64,** No. 5 pp. 2421 - 2434 (2021)

Egyptian Journal of Chemistry

http://ejchem.journals.ekb.eg/

Electrochemical Evaluation of Inhibition Efficiency of Some Nonionic Surfactants Based on tolyltriazole Derivatives on The Corrosion of Cu-Zn alloy in seawater

H. Nady[a,b]*, M. M. El-Rabiei[b]*, M. Fathy[b], Mohamed Attia Migahed[c]

[a] *Chemistry Department, College of Science and Arts in Qurayat, Jouf University, Saudi Arabia*

[b] *Chemistry Department, Faculty of Science, Fayoum University, Fayoum-Egypt*

[c] *Department of Petroleum Applications, Egyptian Petroleum Research Institute (EPRI), Cairo-Egypt.*

Abstract

Two nonionic surfactants based on tolyltriazole derivatives namely: 5-methyl-1 Decaethoxide-benzotriazole, TTA (12) and 5-methyl-1 Tetracosaethoxide-benzotriazole, TTA (24) were synthesized and evaluated as corrosion inhibitors for 65Cu-35Zn alloy dissolution in aerated seawater. The corrosion inhibition capability of these nonionic surfactants has been investigated in seawater solution using potentiodynamic polarization, electrochemical impedance spectroscopy, EIS, and scanning electron microscopic SEM/EDX measurements. According to both potentiodynamic polarization and EIS measurements, it has been found that the investigated tolyltriazoles compounds, TTAs, work as efficient inhibitors for 65Cu-35Zn corrosion and the protection aptitude raised by increasing the concentration of inhibitors. EIS measurements indicated that the charge-transfer resistances increase upon increasing the TTAs concentration. It was found that the percentage inhibition efficiency (η%) increases by increasing the inhibitor concentration. Also, the results showed enhancement in inhibition efficiencies with decreasing the molecular size of the surfactant or the degree of ethoxylation at low concentration. At high concentration, the inhibition efficiency of the different inhibitors independent on the degree of ethoxylation. Potentiodynamic polarization curves indicated that the inhibitors under investigation act as mixed type. Finally, the surface characterization of the protective film formed on 65Cu-35Zn surface was examined by using SEM and energy dispersive X-ray, EDX, techniques. Adsorption of TTA, TTA(12), TTA(24) on the surface of Cu-35Zn in seawater, follows the Langmuir adsorption isotherm. The adsorption free energy of inhibitors on 65Cu-35Zn alloy reveals a strong physical adsorption of the inhibitor on the metal surface..

Keywords: Tolyltriazole; Corrosion; Inhibition; Brass; Nonionic surfactants; EIS

1. Introduction

Copper and its alloys are widely used as microelectronics, condenser and heat exchanger tubing materials in power plants and other industries due to their low corrosion rate, high electrical and thermal conductivities and joining, fatigue resistance and good mechanical workability [1]. The brass alloys covers a wide range of copper-zinc alloys with differing combinations of properties, including, hardness, machinability, wear resistance, good resistance to corrosion and recyclability. The utilization of seawater solution can be seen as effective method for cooling systems in the industrial application. However, the natural seawater solutions contains some corrosive ions such as Cl^- ion, SO_4^{--} ions, CO_3^{--} ions and organic acids, thus, may causing a range of problems, such as corrosion. Brass is frequently the material to select to make the least costly machined products. However, the Cu and Cu-alloys suffer from heavy corrosion in environment including Cl^- ions. Thus, for the use of Cu and its alloys in aggressive conditions, inhibition of the corrosion should be realized [2,3]. More efforts have been made to inhibit the corrosion of Cu and Cu-alloys. In particular, various organic molecules have been used for the purpose by forming an adsorptive film on the alloy surface through the p-electrons in conjugated bonds and hetero-cycles, and contained

*Corresponding author e-mail: hashem_nady@yahoo.com (H. Nady) mmr01@fayoum.edu.eg (M. El Rabiei)
Receive Date: 27 December 2020, Revise Date: 13 January 2021, Accept Date: 31 January 2021
DOI: 10.21608/EJCHEM.2021.55439.3170

electronegative functional groups. One of the most important used inhibitors for the protection of Cu and Cu- alloys is tolyltriazole derivatives [4, 5]. In Cl^- containing media, the corrosion of Cu-Zn alloys takes place by the dissolution of zinc into the electrolyte. There are two types of corrosion: Layered type and local corrosion [6]. The corrosion of the surface takes place all over the surface and is generally observed in Cu-Zn alloys rich in zinc. In local corrosion there are holes and small local pits formed on the surface of the alloy, and there is very little corrosion on other parts of the alloy surface. The surface region has a porous structure and is highly weakened where these pits and holes are formed. The metal surface is easily broken from these regions. Surface film consists of ZnO and Cu_2O in 0.1 M NaCl [6-8]. A. M. Alsabagh, et. al [9] showed that introducing of ethylene oxides into surfactant molecule (ethoxylation) increases the inhibitive effect of surfactant. The presence of ethylene oxides groups increases the solubility of surfactant and hence the extent of its adsorption on the metal surface increases and consequently its protective action improves. Many studies on the inhibition of the corrosion of carbon steel by ethoxylated surfactants have been carried out in different corrosive environment [10-12]. In this work, two of ethoxylated tolyltriazole non ionic surfactants namely; TTA (12) and TTA (24) (*Cf.* Fig. 1), were synthesized as promising corrosion inhibitors for Cu-35Zn alloy in seawater. Potentiodynamic polarization curves and EIS were measured to evaluate the inhibition efficiency of the inhibitors and the results were confirmed by surface study. The surface morphologies in absence and presence of the investigated inhibitor were characterized by SEM/EDX. The chemical structures of the synthesized compounds were confirmed using elemental analysis, FTIR and 1H NMR spectroscopy [13].

2. Experimental details

65Cu-35Zn rod was used as the working electrode. Complete analysis of the chemical composition of the 65Cu-35Zn alloy is given in Table 1. The surface of the 65Cu-35Zn alloy was mechanically sequentially polished prior to use with 400, 600, 1000, 1200 and 2500 grade of emery papers, washed with deionized water, and dried with soft paper, followed by immediate immersion in the test solution. The 65Cu-35Zn sample for electrochemical measurements was spot-welded to Cu wire for electrical contact and was then embedded with epoxy, leaving a surface area of 0.2 cm^2 exposed to the corrosive solutions.

All experiments were carried out in natural seawater solution with and without different concentrations of TTA, TTA (12) and TTA (24) as corrosion inhibitors. Complete chemical composition of seawater (as ions, Conc. /(g/L)) used in this work is: Na^+: 11.33, Ca^{2+}:0.48, Mg^{2+}:1.41, Cl^-: 20.8, SO_4^{--}: 1.92, HCO_3^-: 0.39 and T.D.S. ions: 36.8. The concentration of the synthesized inhibitors was ranged from 50 to 400 ppm. All tests were done under naturally aerated conditions.

The potential of 65Cu-35Zn electrode in seawater were measured versus saturated calomel electrode (SCE) in the absence and presence of different concentrations of TTAs inhibitors. Potentiodynamic polarization studies were carried out using Volta lab 10 PGZ100 "*All-in-one*" potentiostat/galvanostat workstation controlled by Tacussel corrosion analysis software model (Volta master 4). at a scan rate of 10 mV S^{-1} under static condition. In addition, corrosion current density, i_{corr}, and the corrosion potential, E_{corr}, were calculated by Tafel extrapolation technique. Traditional three-electrode system was applied in the measurements: the 65Cu-35Zn specimen as the working electrode, a platinum (Pt) electrode as the auxiliary electrode, and a saturated calomel electrode (SCE) as reference electrode. All the experiments were conducted at room temperature of 298 ± 1 K except in case of studying the effect of temperature. Open circuit potential measurements, E_{OCP}, were performed for approximately 3 h.

EIS measurements were performed at open circuit potential on the 65Cu-35Zn electrode, E_{corr}, by means of impedance equipment Volta lab PGZ 100 potentiostat/galvanostat. Impedance spectra were obtained in the frequency range 0.01 Hz to 100 kHz with the ac voltage amplitude of 10 mV for the sine wave signal.

The surface morphology of the 65Cu-35Zn specimens was examined using the Scanning Electron Microscope (SEM) Model Quanta 250 FEG (Field Emission Gun) attached with EDX Unit, with accelerating voltage 30 K.V., magnification14x up to 1000000 and resolution for Gun.1n. As a type of spectroscopy, relies on the investigation of sample through interaction between the mater and electromagnetic radiation. So that a detector was used to convert X-rays energy into voltage signals. This information is sent to a pulse processor, which measures the signals and passed them into an analyzer for data display and analysis [14]. The synthesized structures of the inhibitor molecules were identified by IR and ^{1}H NMR spectroscopic analyses. Fig. 2 show ^{1}H NMR spectrum of the synthesized inhibitors and their chemical structures.

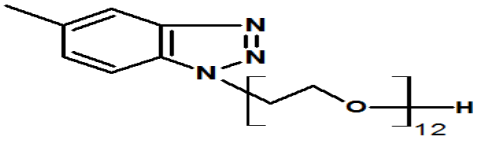

5-methyl-1 Decaethoxide-benzotriazole

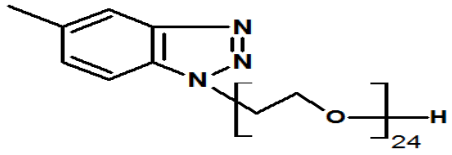

5-methyl-1 Tetracosaethoxide-benzotriazole

Fig. 1. The molecular structures of the two inhibitors, 5-methyl-1 Decaethoxide-benzotriazole (TTA (12)) and 5-methyl-1 Tetracosaethoxide-benzotriazole, TTA (24).

Table 1 - Mass spectrometric analysis for Cu-35Zn electrode material in mass%.

Materials	Cu	Al	Ni	Zn	Mn	Sn	Fe	Si	Mg
Cu-35Zn	65.07	0.311	0.219	33.73	0.0173	0.315	0.232	0.093	0.0106

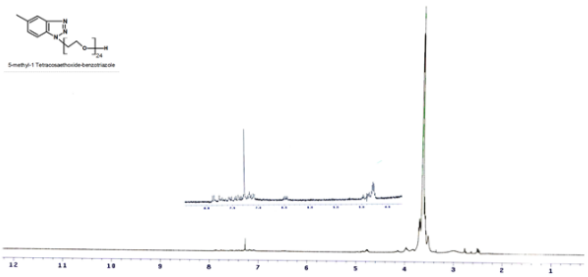

Fig. 2. ^{1}H NMR spectrum of TTA(24) inhibitor.

3. Results and discussion

3.1. Open-circuit potential measurements, OCP.

The effect of the synthesized TTAs inhibitors addition on the corrosion inhibition of 65Cu-35Zn alloy was evaluated by immersion in seawater solution, with the OCP monitored as a function of exposure time. The open circuit potential, *E*ocp,- time response measured for 65Cu-35Zn alloy under the same operating conditions were similar, in the meaning of the potential changing towards the positive values immediately after immersion. After immersion for 40 min, the steady potential is reached for the three systems and then maintained this potential. This behavior is represented by the curves shown in Figs. 3a, b and c. Interaction between the electrolyte and the metal surface occurred, leading to the healing and further thickening of the formed oxide film. This continued until the film acquired a thickness that is stable with respect to the exposure environment. During this stage oxidization of the metal surface is anodic controlled through either an increase in the self-polarization of the anodic areas or a decrease in the self-polarization of the cathodic ones. Addition of the TTAs inhibitors causes the potential of the 65Cu-35Zn electrode to shift into the positive direction to reach steady-state value, E_{ss}. This behavior could be attributed to a decreased rate of metal dissolution by adsorption of TTAs or their protonated forms on the metal surface [15-20].

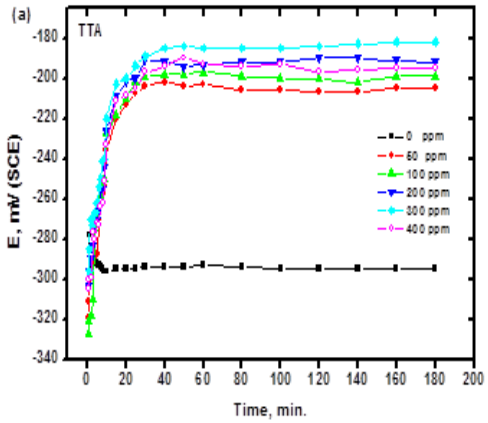

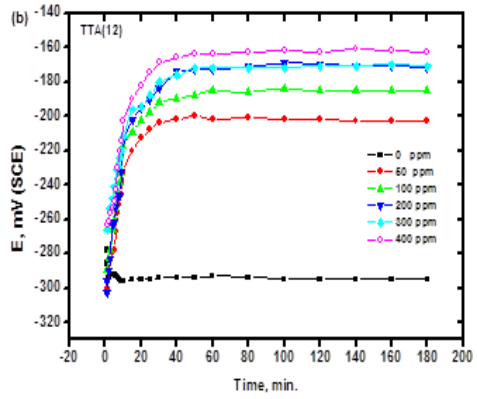

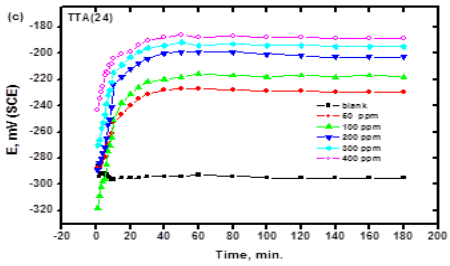

Fig. 3. Open circuit potentials of Cu-35Zn in The Mediterranean seawater, in the absence and presence of different concentration of inhibitors. (■) Free; (●) 50 ppm; (▲) 100 ppm; (▼) 200 ppm; (♦) 300 ppm and 400 ppm (○). (A) TTA ; (B) TTA(12) and TTA(24).

3.2 Potentiodynamic polarization measurements

To examine the corrosion inhibition mechanism, the *E–i* curves for the 65Cu-35Zn were measured by linear potential sweep at scan rate of 10 mV s^{-1} in seawater after the electrode had been immersed for 60 min. Fig. 4a, b and c illustrates the potentiodynamic polarization curves of 65Cu-35Zn alloy in seawater solution in absence and presence of different concentrations of TTAs compounds at 25 ^{o}C. The curves were analyzed by Tafel extrapolation, and the various parameters such as corrosion potential, E_{corr}, and corrosion current density, i_{corr}, were calculated and summarized in Table 2. The values of the inhibition efficiency, η, surface coverage, Θ, and covered surface areas were calculated and tabulated in the same Table. With increasing the concentration of three inhibitors in the corrosive solutions, the anodic and cathodic curves move directly to lower values of current densities, and the corrosion rate of 65Cu-35Zn alloy has been decreased significantly. This mean that, the investigated inhibitors work primarily at the electron sink areas to hinder the oxidation of alloy components, and secondarily preventing the reduction of oxygen. Each curve in Fig. 4 is nearly parallel with the others, which indicates that the mechanism of the anodic and cathodic reactions is not changed by the addition of these compounds, and the corrosion processes are controlled just by restraining the rates of reactions [21,22]. The values of the η, surface coverage and covered surface area are dependent on both the inhibitors structure and its concentration as presented in Table 2. The degree of surface coverage (θ) and the percentage inhibition efficiency (η%) were calculated using the following equations [23]: $\Theta = 1 - i_{inh}/i_{corr}$ and $\eta\ \% = [1 - i_{inh}/i_{corr}]\ \%\ 100$, where i_{corr} and i_{inh} are the corrosion current densities in the absence and presence of the inhibitor, respectively. The variation of the corrosion inhibition efficiency, η, with the inhibitor concentration for the three investigated inhibitors was explained in Fig. 5. From the data obtained in Table 2, it can be seen that the values of i_{corr} are greatly decreased in the presence of the inhibitors, and the inhibition efficiencies calculated from i_{corr} increase with the concentration of these compounds. The η % values of TTA, TTA(12) and TTA(24) at each concentration are extremely high, and the maximum values of the efficiencies are 91% with TTA, 94% with TTA(12) and 92% with TTA(24) at the 400 ppm within the concentration range of our research. The shift of β_a and β_c indicate that the oxidizing dissolution as well as the oxygen reduction is suppressed by the adsorption of TTAs compounds. Therefore, it confirms that these compounds act as mixed-type corrosion inhibitors which suppress both anodic and cathodic reaction by adsorbing on the Cu surface [24]. When Polarization curves of 65Cu-35Zn in seawater without and with different concentration of inhibitors (TTA, TTA(12) and TTA(24)) at 298K are compared with each other, it was noticed that i_{corr} in case of using TTA is lower than TTA (12) and TTA(24) (*cf*. Fig. 5). This could be attributed to steric effect of ethylene oxide units of inhibitor molecules. Particularly, at the concentration of 400 ppm, the inhibition efficiencies of TTA (12) is higher than that recorded in case TTA and TTA(24) inhibitors (*cf*. Fig. 5). Fig. 6 shows the polarization curves of 65Cu-35Zn after immersion in seawater solution containing three investigated inhibitors at the concentration of 300 ppm. The presence of inhibitors evidently suppresses both the anodic and cathodic reactions while the anodic branches are retarded to the larger extent.

The corrosion rate measurements indicate that Cu has lower corrosion rates when alloyed with zinc which is attributed to the formation of stable Zinc oxide at the electrode surface [7, 8]. It has been generally accepted that the corrosion of freshly polished Cu and Cu-based alloys in naturally aerated neutral Cl^- solutions involves the cathodic reduction of oxygen, according to [25-28]: $O_2 + 2\ H_2O + 4e^- \rightarrow 4OH^-$. The major anodic reaction is the Cu dissolution according to the following equation [29,30]: $Cu + 2Cl^- \rightarrow CuCl_2^- + e^-$. It was suggested that the presence of $CuCl_2^-$at the electrode surface leads to a hydrolysis reaction and the formation of Cu_2O [29] according to: $2CuCl_2^- + H_2O \rightarrow Cu_2O + 4Cl^- + 2H^+$. In the Zn containing alloys an additional passivation process is taking place due to the formation of Zn-oxide film during a dezincification process according to [28,31]: $Zn + H_2O \rightarrow ZnO + 2H^+ + 2e^-$. The addition of

alloying element as Zn improves the corrosion resistance of Cu due to the formation of a compact Zn oxide layer. The compositions of the barrier CuO layers formed on pure Cu and the 65Cu-35Zn alloy are obviously not identical. The barrier Cu_2O layer is a p-type semiconductor containing cation vacancies as the main defects [32]. NiO is also a p-type semiconductor, whereas ZnO is an n-type semiconductor, with a band gap of 3.2 eV [32]. According to the Solute Vacancy Interaction Model (SVIM) [33] the beneficial effect of a Ni addition to copper has been interpreted in terms of the segregation of the alloying element (Ni), the formation of charge solutes and their subsequent complexation with mobile cation vacancies [34]. In analogy with Cu_xNi alloys, zinc ions may be incorporated into cation vacancies normally present in the deficient structure of Cu_2O. Charged solutes would interact electrostatically with oppositely charged mobile cation vacancies: $Zn_{Cu}^{\bullet}$(ox) + $V_{Cu}^{'}$ (ox) = [$Zn_{Cu}V_{Cu}$]. This reaction leads to the formation of a neutral species and thus to a decreased number of cation vacancies.

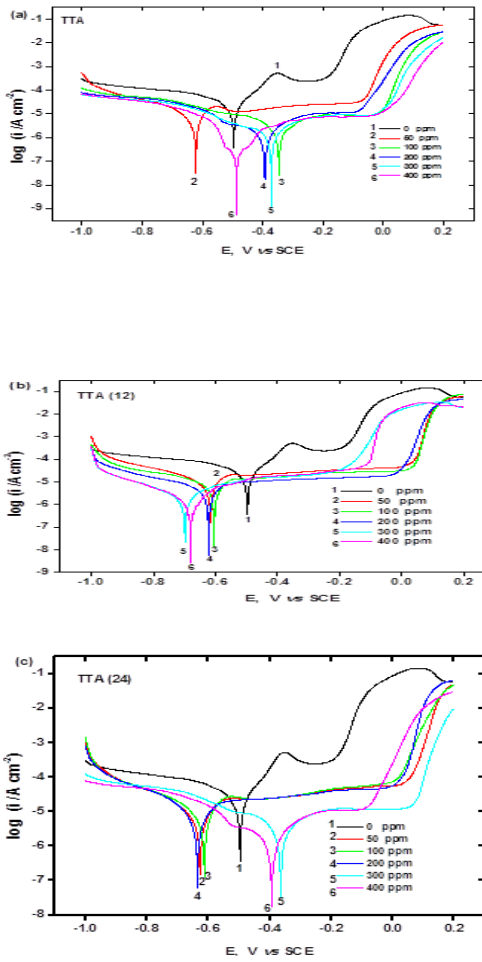

Fig. 4. Potentiodynamic polarization of Cu-35Zn in absence and presence of different concentrations of different inhibitors in naturally aerated stagnant sea water at 25 °C. (a) TTA, (b) TTA(12) and (c) TTA(24).

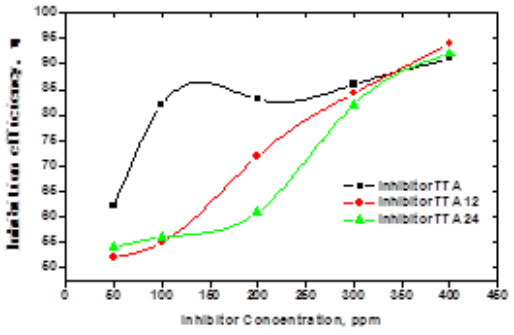

Fig. 5. Variation of the corrosion inhibition efficiency, η, of the alloy corrosion in stagnant naturally aerated seawater solution with the inhibitors concentration at 25◦C.

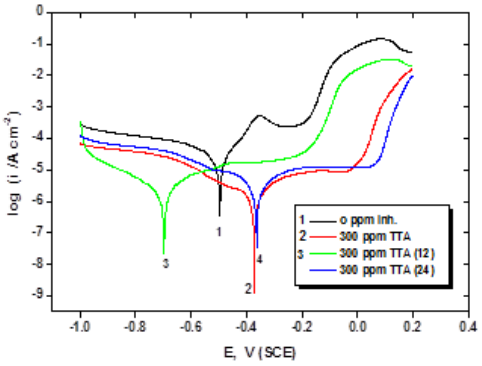

Fig. 6. log *i*–*E* curves of Cu-35Zn in absence and presence of 300 ppm of different inhibitors in naturally aerated stagnant sea water at 298 K. (1) blank, (2) TTA, (3) TTA(12) and (4) TTA(24).

Adsorption isotherm

A different adsorption isotherm models such as Langmuir, Frumkin and Temkin have been used to describe the adsorption behavior of the studied inhibitors. The adsorption behavior of TTAs inhibitors is tested with these isotherms and found well fitted with Langmuir isotherm. The protection efficiency of organic inhibitor molecules mainly depends on their adsorption ability at the metal surface/solution interface which occur by the replacement of H_2O molecules by inhibitor molecules according to the following equation [35-38]: Org(sol) + xH_2O(ads)↔Org(ads) + xH_2O(sol), where Org(sol) and Org(ads) are the organic inhibitor

molecules in the solution and adsorbed on the metallic surface, respectively. Electrochemical results are involved to study the adsorption of TTAs on the 65Cu-35Zn surface. To investigate the nature of the adsorption mode of the surfactants, the data of surface coverage data, θ, as a function of inhibitor concentration was calculated at 298 K. Experientially, applied assumption that surface coverage Θ ≈ η % looks reasonable, although almost linear function exists between them. Therefore, the surface coverage Θ is defined as η % in the following discussion. The surface coverage (Θ) was calculated from the corrosion current densities obtained from polarization results, where i_{inh} and i_{corr} are the corrosion current density for 65Cu-35Zn alloy in the presence and absence of TTAs compounds in the seawater, respectively. Results reveal that the Langmuir isotherm provides the best description for the adsorption behavior of TTAs, $K_{ads}.C = \frac{\theta}{1-\theta}$. Here K_{ads} is the equilibrium constant of the inhibitor adsorption process, C is the inhibitors concentration. Fig. 7 shows straight line plots for C_{inh}/θ vs. C_{inh} (concentration of ATTs) a 25ºC. The linear correlation coefficient (*R*) values is almost equal to 1, suggesting that the adsorption of TTAs inhibitors on the 65Cu-35Zn alloy obeys the Langmuir adsorption model. According to Langmuir adsorption isotherm, the relation of the equilibrium constant for the adsorption process, $K_{ads,}$ to the standard free energy of adsorption ΔG^0_{ads} can be expressed by the following equation [39,40]: $K_{ads} = \frac{1}{55.5}\exp[(-\Delta G^{o}_{ads}{}^{\circ})/RT]$. K_{ads} values can be calculated from the intercepts of the straight lines on the C/θ axis. The value 55.5 is the concentration of water in solution expressed in mol/L scale. The value of adsorption free energy, ΔG^0_{ads}, for each investigated inhibitor are listed in Table 3. The addition of the investigated surfactants caused negative values of the free energy of adsorption which indicated that these inhibitors were adsorbed spontaneously on the 65Cu-35Zn surface. It has been a matter of common practice that if the absolute value of ΔG^0_{ads} is lower than 40 kJ/mol, the type of adsorption is regarded as physisorption, and the corrosion inhibition takes action due to the electrostatic interactions between the charged molecules and the charged metal. If the absolute value of ΔG^0_{ads} is higher than 40 kJ/mol, it functions by chemisorption due to the covalent bond formed by the charge sharing or a charge transfer from the inhibitor molecule to the metal surface [41-44]. From the data presented in Table 3, the calculated values of ΔG^0_{ads}, the three inhibitors are absorbed by physisorpion.

Table 2: Polarization parameters and rates of corrosion of Cu-35Zn alloy in absence and presence of different concentrations of TTA, TTA(12) and TTA(24) in naturally aerated stagnant sea water at 25 ˚C

Concn ppm	E_{corr} mV	i_{corr} μA cm^{-2}	β_a mV	B_c mV	Corr. rate /μmy^{-1}	Surface coverage ?	Surface area (cm^2)	? %
Inhibitor 1 TTA								
0	-490	4.6	77	-108	53.9	---	---	---
50	-616	1.77	61	-77	21	0.615	0.123	62
100	-341	0.81	65	-86	9.6	0.824	0.164	82
200	-389	0.76	91	-141	9	0.834	0.167	83
300	-369	0.65	89	-135	7.7	0.858	0.172	86
400	-485	0.43	122	-88	5	0.906	0.181	91
Inhibitor 2 TTA(12)								
50	-611	2.2	59	-84	25.5	0.521	0.104	52
100	-600	2.09	60	-91	24.6	0.546	0.109	55
200	-618	1.3	55	-93	15.7	0.717	0.143	72
300	-692	0.58	58	-83	6.9	0.873	0.175	87
400	-675	0.26	45	-39	3.1	0.943	0.189	94
Inhibitor 3 TTA(24)								
50	-623	2.1	57	-81	24.9	0.543	0.109	54
100	-608	2.01	57	-78	23.8	0.563	0.113	56
200	-631	1.79	64	-71	21	0.611	0.122	61
300	-360	0.85	65	-77	10	0.815	0.163	82
400	-389	0.33	43	-84	3.8	0.917	0.183	92

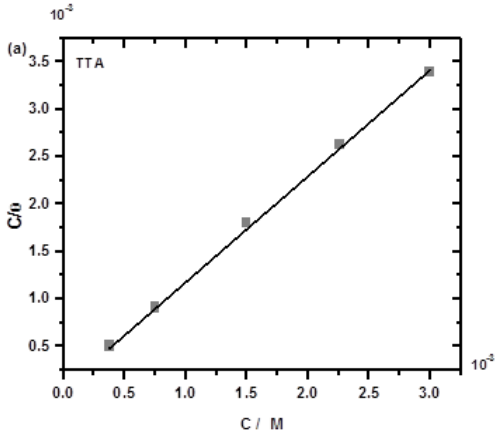

Table 3 : The values of adsorption free energy, ΔG^0_{ads} , for the different inhibitors.

Alloy	ΔG / KJ mol^{-1}		
	TTA	TTA(12)	TTA(24)
Cu-35Zn	-35.0	-33.1	-32.9

Table 4: Activation energy, E_a, and ΔS_a for the corrosion of Cu-35Zn in sea water at 300 ppm of TTAs concentration.

inhibitor	Ea / kJ mol^{-1}	ΔS_a / J K^{-1} mol^{-1}
TTA	19.8	210.7
TTA(12)	18.3	182.6
TTA(24)	16.2	97.7

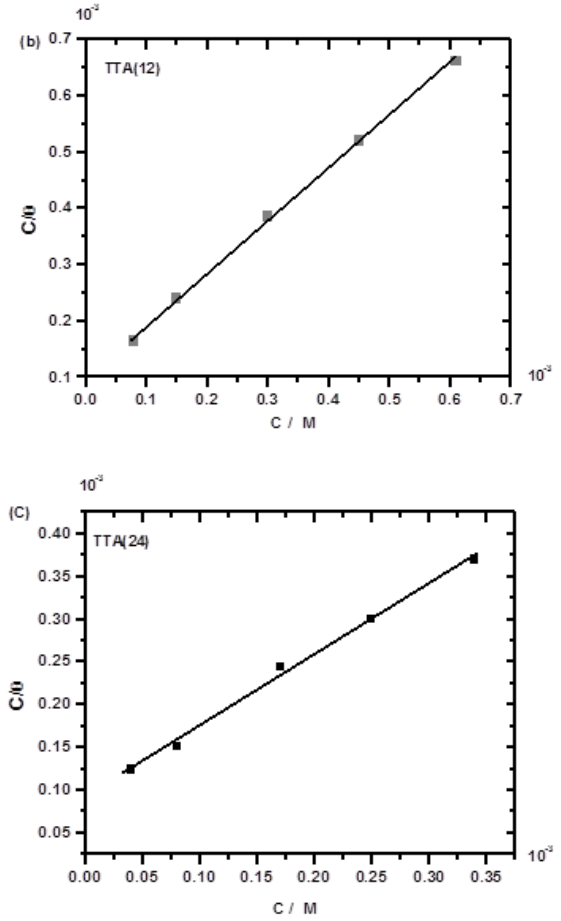

Fig. 7. Langmuir adsorption isotherm of TTA (a), TTA(12) (b) and TTA(24) (c) on the surface of Cu-35Zn in The Mediterranean seawater at 298 K.

Effect of temperature

Fig. 8a presents the effect of electrolyte temperature on the dissolution rate of 65Cu-35Zn alloy in seawater in the presence of 300 ppm TTA(24) as a representative sample. It can be seen from Fig. 8a that increasing solution temperature increases the i_{corr} of the polarization curves. The value of i_{corr} increases with increasing the solution temperature, indicating that the corrosion rate of 65Cu-35Zn in seawater is accelerated by the rise in temperature. The effect of solution temperature on the corrosion rate can be expressed by the Arrhenius equation: i_{corr} = A exp (-*E*a/RT), where A and Ea are pre-exponential factor and apparent activation energy of the metal dissolution reaction, respectively. The Arrhenius plots are illustrated in Fig. 8b. Fig. 8b shows straight lines of log i_{corr} versus 1/T for seawater in the presence of 300 ppm of different inhibitors and the values of *E*a can be determined from the slopes. Calculated activation energies for the corrosion process in presence of TTA, TTA(12) and TTA(24) are presented in Table 9. As the solution temperature increases, the activation energy decreases which means that the protection efficiency decreases as the solution temperature increase. The decrease in corrosion rate upon adding surfactants to seawater solution is due to the increase of apparent activation energy. From Table 4, the calculated values of *E*a was found to be increasing in the following direction: TTA > TTA(12) > TTA(24).

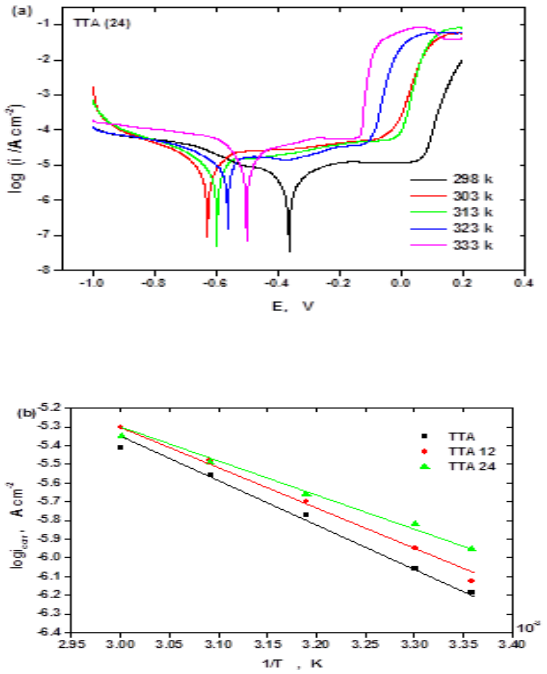

Fig. 8. (a) Effect of temperature on the polarization curves in seawater solutions containing 300 ppm of the different inhibitors. (b) Arrhenius slopes calculated from corrosion current density for Cu-35Zn in seawater solutions containing 300 ppm of the different inhibitors.

The electrochemical impedance measurements, EIS.

EIS measurements on the Cu-35Zn electrodes in seawater alone and in the presence of various concentration of the three inhibitors were performed at the E_{ocp}. Fig. 9 represents the influence of TTA, TTA(12) and TTA(24) compounds at different concentrations on impedance plots of Cu-35Zn presented in the form of Bode plot, which display the relationship between impedance magnitude, |Z|, phase angle, ɵ, and log *frequency*, log *f*. A rough inspection of the EIS spectrums shows that mass transport taking place through the phase layer must

be taken into account and that the corresponding equivalent circuit of the system must contain more than one time constant. All Bode spectrums, show two phase maxima at intermediate and low frequencies. The absence of the impedance plateau and the presence of a second phase maximum at low frequencies indicate the presence of a diffusion process [45]. From Fig. 9, the phase angles of the 65Cu-35Zn alloy in inhibitor-containing solutions are evidently bigger than that in inhibitor-free solutions in the low and high frequency region. A much wider frequency range for the alloy in inhibitor-containing solutions suggests that the protective layer can maintain its characteristic response over a longer period of immersion time. The semi-circle size of Nyquist plots increase by increasing inhibitor concentration. This means that the increase in the TTAs concentration increases the impedance value, indicate that the inhibitor molecules inhibit dissolution of Cu-35Zn alloys in seawater by adsorption mechanism [46], which is consistent with the results of the polarization experiments. The impedance data were analyzed using the software provided with the impedance system, where the dispersion formula was used. For a simple equivalent circuit model consisting of a parallel combination of a capacitance, C_{dl}, and a resistor, R_{ct}, in series with a resistor, R_s, representing the solution resistance, the electrode impedance, Z, is represented by the mathematical formulation: $Z = R_s + \frac{R_{ct}}{1+(2\pi f R_{ct} C_{dl})^{\alpha}}$, where α denotes an empirical parameter ($0 \leq \alpha \leq 1$) and f is the frequency in Hz. The above relation is known as the dispersion formula and it takes into account the deviation from the ideal RC-behavior in terms of a distribution of time constants due to surface inhomogeneties, roughness effects and variations in properties or compositions of surface layers [47,48]. To account for the diffusion process and surface film the impedance data of the alloy in different inhibitor concentrations were analyzed using the equivalent circuit shown in Fig. 10, where another $R_{pf}C_{pf}$ combination and was introduced to account for the spontaneously formed passive film. The calculated equivalent circuit parameters for the alloy in different inhibitor concentration contents were presented in Table 6. From Table 6, the EIS results indicate the formation and protective effects of the inhibitor-adsorptive film on alloy surface, and its contribution to increasing corrosion resistance of the Cu-Zn alloy. From EIS data it was found that R_{ct} and R_f value of inhibitor TTA is greater than that of inhibitors (TTA(12) and TTA(24)), indicating higher inhibition efficiency than the other two inhibitors (cf. Fig. 11). The data obtained from EIS are in a good agreement with aforementioned results of potentiodynamic polarization measurements. The Cu-35Zn alloy sample was immersed in seawater solution containing 300 ppm of each inhibitor, and the impedance measurements were measured every several hours. The EIS spectra obtained with 300 ppm TTA at different intervals of electrode immersion are presented as Bode and Nyquist plots in Fig. 12(a,b,c). In the immersion time, the surfactants molecules adsorbed physically on the Cu-35Zn alloy surface, then TTAs molecules combined into compounds with Cu ions and deposited on the alloy surface, gradually forming the protective layer. From Fig. 12, the low-frequency limits of impedance modulus (|Z|) progressively increase with time of immersion. The evolution of impedance plot in terms of shape and size at different immersion times demonstrates that the barrier film on the electrode surface is thickened and that protection afforded by corrosion product film [49]. The EIS spectra were further analyzed by fitting with the equivalent circuit shown in Fig. 10. The EIS data obtained at different time of electrode immersion in seawater at a certain concentration of different inhibitors are summarized in Table 7. In the initial 3 h from electrode immersion, the barrier film resistance, R_f, values increased slowly (see Fig. 12C), which indicated that the protective layer was formed gradually. During 3 h to 5 h, the R_f value increased rapidly, indicating that the surfactant molecules adsorbed on the alloy surface were high enough to form a barrier layer much faster than the damage by corrosive ions; and the protective layer became continuous and complete. In case TTA inhibitor, the R_f values increased slowly (from 165.5 kΩ cm^2 to 186.3 kΩ cm^2) during the initial 3 h from electrode immersion and then increased rapidly (from 186.3 kΩ cm^2 to 453.6 kΩ cm^2), which was related to the formation of the protective layer.

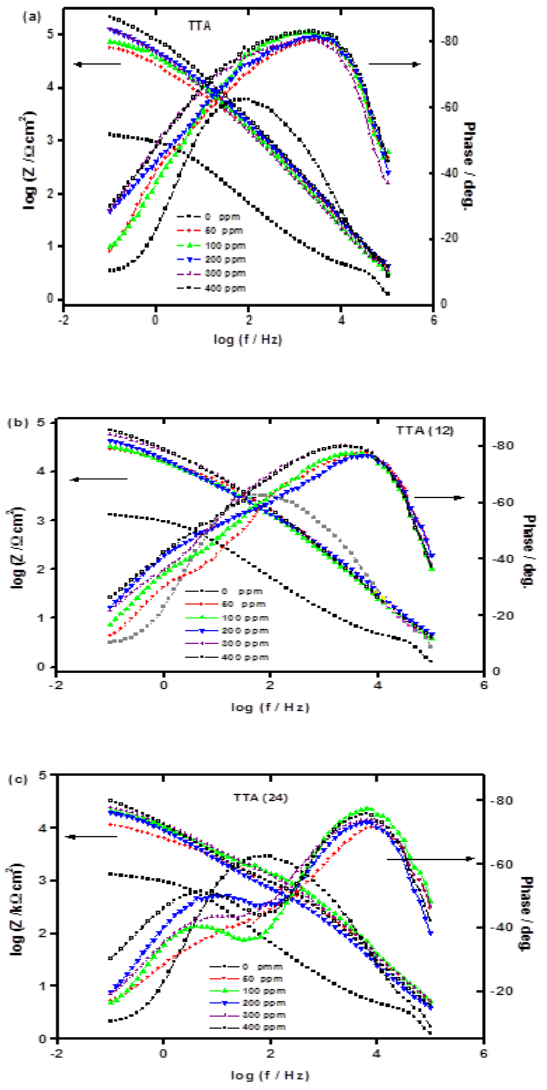

Fig. 9. Bode plots of Cu-35Zn alloy in natural aerated seawater with different concentrations of inhibitor TTA(12).

Table 5: Equivalent circuit parameters of Cu-35Zn electrode in absence and presence of different concentrations of TTA, TTA(12) and TTA(24) in naturally aerated stagnant sea water at 25 ˚C.

Conc / ppm	R_s /Ω	R_{ct} /kΩ cm^2	C_{dl} /mF cm^{-2}	α_1	R_f /kΩ cm^2	C_f /mF cm^{-2}	α_2
Inhibitor 1 TTA							
0	1.5	1.3	60 x10^{-3}	0.99	----	----	----
50	2.5	7.8	0.32 x 10^{-3}	0.99	70.9	5.6 x10^{-3}	0.99
100	7.6	11.3	0.29 x10^{-3}	0.99	80.8	2.5 x10^{-3}	0.99
200	13.4	19.5	0.21 x 10^{-3}	0.99	152.1	1.3 x10^{-3}	0.99
300	9.3	22.6	0.28 x10^{-3}	0.99	165.5	3.1 x10^{-3}	0.99
400	5.0	28.3	0.12 x10^{-3}	0.99	219.7	2.3 x10^{-3}	0.99
Inhibitor 2 TTA (12)							
0	1.5	1.3	60 x10^{-3}	0.99	----	----	----
50	3.1	8.8	0.29 x10^{-3}	1	37.4	8.5 x10^{-3}	0.99
100	11.9	8.1	0.98 x10^{-3}	0.99	75.5	14.0 x10^{-3}	0.99
200	11.2	10.5	0.61 x10^{-3}	0.99	71.1	14.1 x10^{-3}	1
300	16.8	11.8	0.27 x10^{-3}	0.99	72.6	5.5 x10^{-3}	0.99
400	3.2	13.6	0.29 x10^{-3}	0.99	92.1	3.5 x10^{-3}	0.99
Inhibitor 3 TTA (24)							
0	1.5	1.3	60 x10^{-3}	0.99	----	----	----
50	4.8	2.5	0.63 x10^{-3}	0.99	17.8	35.7 x10^{-3}	0.99
100	4.3	2.3	0.68 x10^{-3}	0.99	25.0	15.9 x10^{-3}	0.99
200	1.8	1.7	0.96 x10^{-3}	0.99	26.5	24.0 x10^{-3}	1
300	2.8	3.0	0.53 x10^{-3}	0.99	34.5	18.4 x10^{-3}	0.99
400	2.6	1.8	0.86 x10^{-3}	0.99	58.2	17.3 x10^{-3}	1

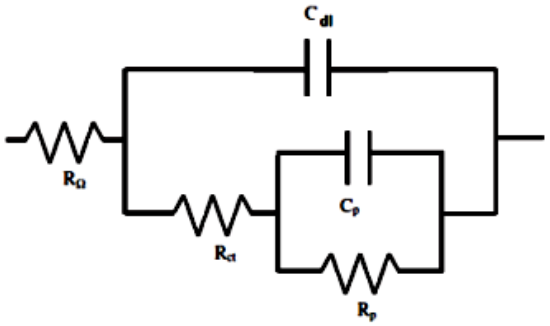

Fig. 10. Equivalent circuit model used in the fitting of the impedance data of Cu and Cu-alloys at different conditions, R_s = solution resistance, R_{ct} = charge-transfer resistance, C_{dl} = double layer capacitance, R_{pf} = passive film resistance, and C_{pf} = passive film capacitance.

Table 6: Effect of time on Cu-35Zn electrode immersed in 300 ppm TTA (a), TTA(12) (b) and TTA(24) (c) in naturally aerated stagnant sea water at 25 ˚C.

Time / hrs	R_s /Ω	R_{ct} /kΩ cm^2	C_{dl} /mF cm^{-2}	α_1	R_f /kΩ cm^2	C_f /mF cm^{-2}	α_2
Inhibitor 1 TTA							
1	9.3	22.6	0.28 x10^{-3}	0.99	165.5	3.1 x10^{-3}	0.99
2	3.4	27.6	0.73 x10^{-3}	0.99	175.6	1.8 x10^{-3}	0.99
3	6.2	34.6	0.46 x10^{-3}	0.99	186.3	0.72 x10^{-3}	0.99
4	3.02	40.6	0.32 x10^{-3}	0.99	257.1	0.62 x10^{-3}	0.98
5	5.1	39.4	0.26 x10^{-3}	0.98	453.6	0.88 x10^{-3}	0.99
6	4.9	44	0.36 x10^{-3}	0.98	422.8	1.2 x10^{-3}	0.98
Inhibitor 2 TTA(12)							
1	16.8	11.8	0.27 x10^{-3}	0.99	72.6	5.5 x10^{-3}	0.99
2	43.8	16.1	0.63 x10^{-3}	0.99	85.6	5.8 x10^{-3}	0.99
3	22.9	20.1	0.49 x10^{-3}	0.98	90.1	4.4 x10^{-3}	0.99
4	10.4	25.4	0.25 x10^{-3}	0.99	105	3.1 x10^{-3}	0.99
5	20.8	31.8	0.32 x10^{-3}	0.99	106	3.7 x10^{-3}	0.99
6	19.3	32.1	0.39 x10^{-3}	0.99	118	3.5 x10^{-3}	0.99
Inhibitor 3 TTA(24)							
1	2.8	3.04	0.53 x10^{-3}	0.99	34.5	18.4 x10^{-3}	0.99
2	3.07	1.65	1.5 x10^{-3}	0.99	38.9	25.9 x10^{-3}	1
3	2.4	3.36	0.75 x10^{-3}	0.99	40.7	24.7 x10^{-3}	0.99
4	2.1	3.69	0.68 x10^{-3}	0.99	53.2	23.9 x10^{-3}	0.99
5	2.73	4.31	0.58 x10^{-3}	0.99	68.3	23.3 x10^{-3}	0.99
6	2.1	4.66	0.54 x10^{-3}	0.99	82.4	19.3 x10^{-3}	1

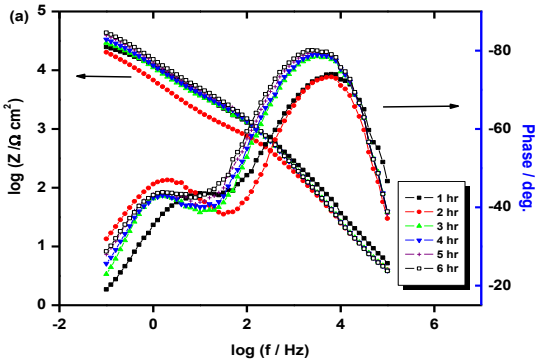

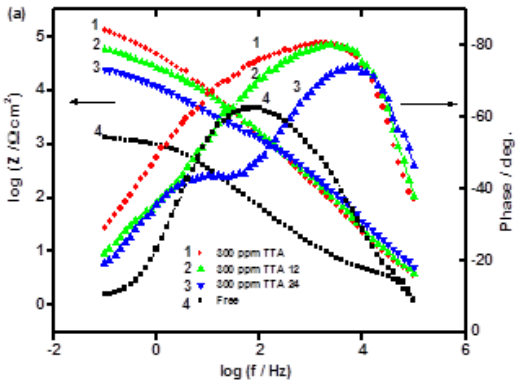

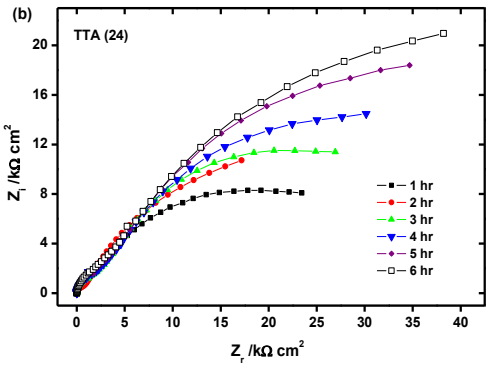

Fig. 11. Bode and Nyquist plots of Cu-35Zn alloy in seawater in absence and presence of 300 ppm of TTA, TTA(12) and TTA(24).

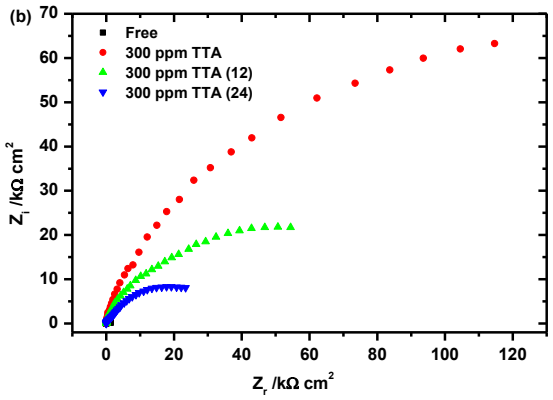

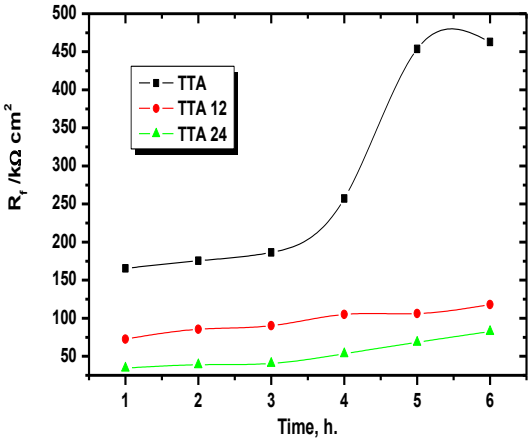

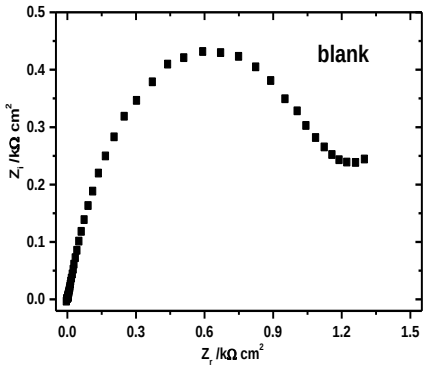

Fig. 12. Bode **(a)** and Nyquist **(b)** plots of the Cu-35Zn alloy recorded at the open circuit potential in aerated seawater containing 300 ppm TTA(24) after different time of immersion. (c) Relationship between surface film resistance, R_f, and the immersion time.

Surface analyses

The surface morphology of a Cu-35Zn sample before immersion in seawater was studied by SEM and EDX analysis as shown in Fig. 13(a, b, c). Before the immersion tests (Fig. 13), the electrode surface was relatively smooth. Figs. 14(a,b, c) shows the characterization of corroded surface after immersion in seawater for 24 h. Compared with the specimen before immersion, the specimen in the seawater without TTA(24) (Fig. 14a) is strongly corroded by the medium, resulting in increasing the corrosion in

boundaries between the elements in alloy and increasing surface roughness. The analysis of the surface composition with EDX confirms the formation of oxides film after electrode immersion in the seawater. Although the oxygen content measurement with EDX may not be very accurate, the presence of oxygen in EDX spectrum is a clear indication of oxidation during the electrode immersion in the seawater solution and the presence of oxide film at the metal surface. In the presence of the TTA(24) inhibitor (Fig. 15), there is much less damage (nearly no damage) on the alloy surface, which further confirm the inhibition action. Therefore, it can be concluded that the TTA inhibitors possesses good inhibiting ability for Cu-Zn corrosion.

Conclusion

1. The synthesized Tolyltriazole compounds were acting as effective inhibitors for Cu-35Zn corrosion in seawater.
2. By analyzing the polarization and EIS results it can be noticed that the corrosion resistance of Cu-35Zn increased with increasing the inhibitors concentration.
3. The data obtained using potentiodynamic polarization measurements and EIS measurements are in good agreement.
4. Long immersion of Cu-35Zn alloy in seawater in presence of tolyltriazole inhibitors improves it corrosion resistance.
5. The adsorption of the inhibitors molecules obeyed the Langmuir adsorption isotherm.
6. The potentiodynamic polarization curves indicated that the inhibitors molecules inhibit both anodic metal dissolution and also cathodic oxygen reduction, so that the studied inhibitors classified as mixed-type inhibitors.
7. Increasing the temperature of the seawater in presence of TTAs has been investigated, showing that the surface coverage of the electrode decrease with increasing temperature.

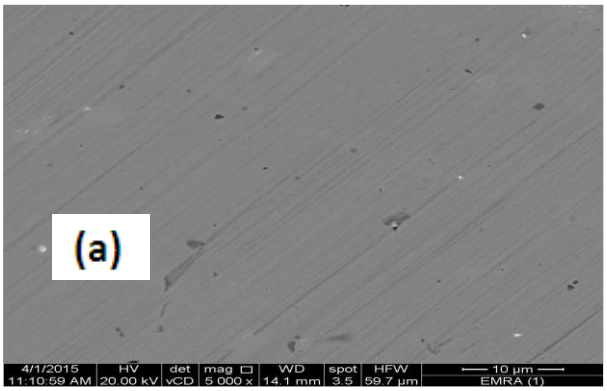

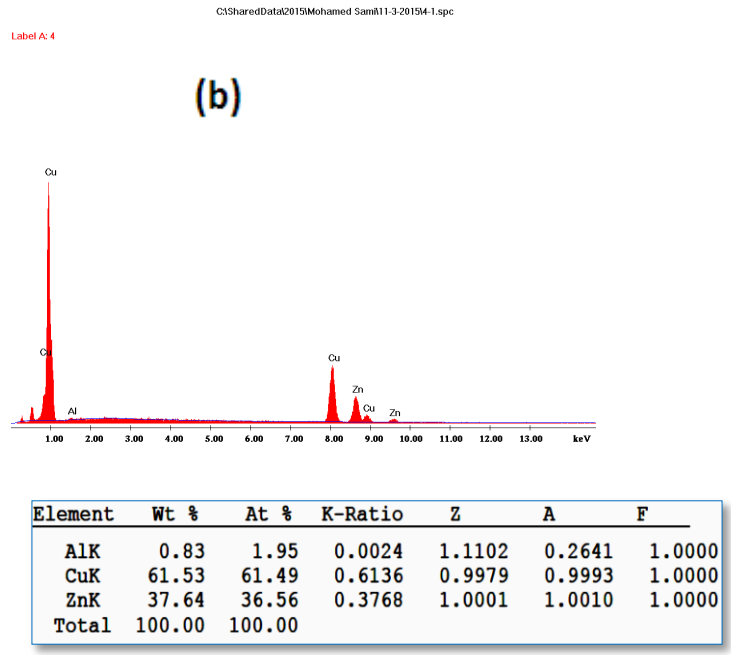

Fig. 13. SEM micrograph (a) and EDX results (b and c) of Cu-Zn alloy before electrochemical testing.

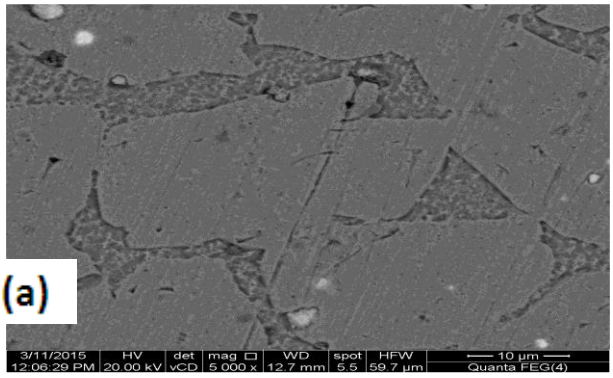

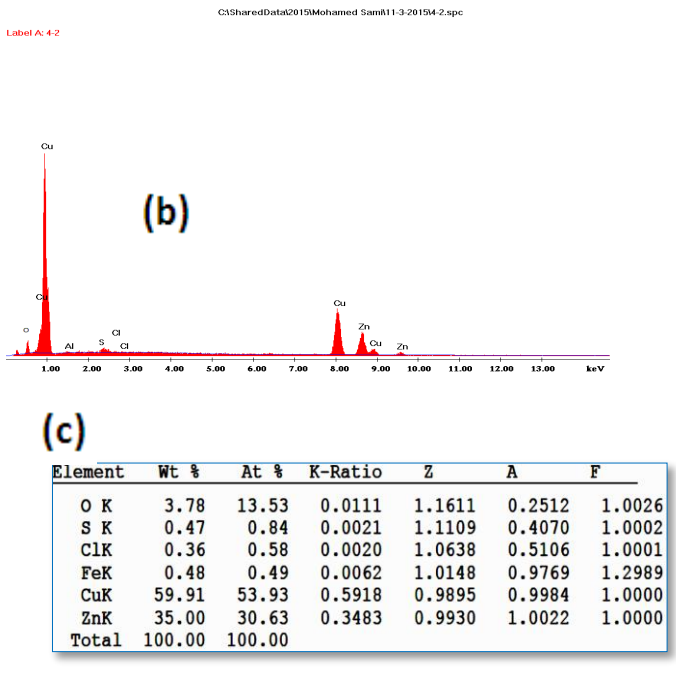

Fig. 14. SEM image of the Cu-Zn alloy surface (a) and EDX results of corrosion (b and c) products after immersion in natural aerated The Mediterranean seawater.

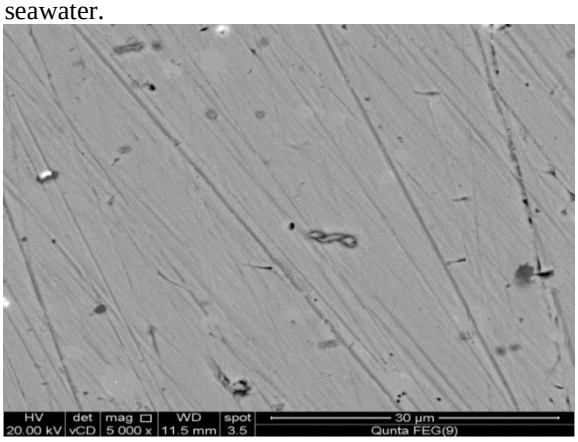

Fig. 15. SEM image of the Cu-Zn alloy surface after immersion in natural aerated The Mediterranean seawater containing 400 ppm of TTA(24).

Conflicts of interest: On behalf of all authors, I confirm that this manuscript has no conflict of interest.

References

[1] Lalitha, A., Ramesh, S., Rajeswari, S. (2005) Surface protection of copper in acid medium by azoles and surfactants. Electrochimica Acta, **51**:47–55.

[2] Liu, T., Chen, S., Cheng, S., Tian, J., Chang, X., Yin, Y. (2007) Corrosion behavior of super-hydrophobic surface on copper in seawater**.** Electrochimica Acta, **52**: 8003-8007.

[3] Otieno-Alego, V., Hope, G.A., Notoya, T., Schweinsberg, D.P. (1996) An electrochemical and sers study of the effect of 1-[N,N-bis-(hydroxyethyl)aminomethyl]-benzotriazole on the acid corrosion and dezincification of 60/40 brass. Corrosion Science, **38:** 213-223.

[4] Tommesani, L., Brunoro, G., Fridnani, A., Montricelli, C., DalColle, M. (1997) On the protective action of 1,2,3-benzotriazole derivative films against copper corrosion. Corrosion Science, **39:** 1221-1237.

[5] El-Naggar, M.M. (2000) Bis-triazole as a new corrosion inhibitor for copper in sulfate solution. A model for synergistic inhibition action. *Journal of materials science,* **35**: *6189*-6195.

[6] Holliday, J.E., Pickering, H.W. (1973) A Soft X-Ray Study of the Near Surface Composition of Cu30Zn Alloy during Simultaneous Dissolution of Its Components. Journal of the Electrochemical Society, **120:** 470-475.

[7] Badawy, W.A., El-Egamy, S.S., El-Azap, A.S. (1995) The electrochemical behaviour of leaded brass in neutral CL− and SO4− media. Corrosion Science, **37**: 1969-1979.

[8] Moralles, J., Fernandez, J. T, Esparza, P., Gonzalez, S., Salvarezza, R. C., Arvia, A. J. (1995) A comparative study on the passivation and localized corrosion of α, β, and α + β brass in borate buffer solutions containing sodium chloride—I. Electrochemical data. Corrosion Science, **37:** 211-229.

[9] Kabasakaloğlu, M., Kıyak, T., Şendil, O., Dinçer, S. (2002) Electrochemical behavior of brass in 0.1 M NaCl. Applied Surface Science, **193**: 167-174.

[10] Alsabagh, A.M., Migahed, M.A., Awad, H. S. (2006) Reactivity of polyester aliphatic amine surfactants as corrosion inhibitors for carbon steel in formation water (deep well water). Corrosion Science, **48**: 813-828.

[11] Migahed, M.A., Abd-El-Raouf, M., Alsabagh, A.M., Abd-El-Bary, H.M. (2005) Effectiveness of some non ionic surfactants as corrosion inhibitors for carbon steel pipelines in oil fields. Electrochimica Acta, **50**: 4683-4689.

[12] Migahed, M.A., Mohamed, H.M., Alsabagh, A.M. (2003) Corrosion inhibition of H-11 type carbon steel in 1 M hydrochloric acid solution by N-propyl amino lauryl amide and its ethoxylated derivatives. Materials Chemistry and Physics, **80:** 169-175.

[13] Migahed, M.A., El-Rabiei, M.M., Nady, H., Fathy, M. (2016) Synthesis, characterization of some ethoxylated tolyltriazole derivatives and evaluation of their performance as corrosion inhibitors for Cu-10Al alloy in seawater. Journal of Environmental Chemical Engineering, **4**: 3741-4752.

[14] Amin, M.A. (2006) Weight loss, polarization, electrochemical impedance spectroscopy, SEM and EDX studies of the corrosion inhibition of copper in aerated NaCl solutions. Journal of Applied Electrochemistry, **36:** 215-226.

[18] Khaled, K. (2010) Electrochemical investigation and modeling of corrosion inhibition of

aluminum in molar nitric acid using some sulphur-containing amines. Corrosion Science, **52**: 2905–2916.

[16] Zhang, Qi., Gao, Z., Xu, F., Zou, X. (2011) Adsorption and corrosion inhibitive properties of gemini surfactants in the series of hexanediyl-1,6-bis-(diethyl alkyl ammonium bromide) on aluminium in hydrochloric acid solution. Colloids and Surfaces A: Physicochemical and Engineering Aspects, **380:** 191– 200.

[17] Safak, S., Duran, B., Yurt, A., Türkoglu, G. (2012) Schiff bases as corrosion inhibitor for aluminium in HCl solution. Corrosion Science, **54:** 251–259.

[18] Yurt, A., Aykin, Ö. (2011) Diphenolic Schiff bases as corrosion inhibitors for aluminium in 0.1M HCl: Potentiodynamic polarisation and EQCM investigations. Corrosion Science, **53:** 3725–3732.

[19] Patel, A.S., Panchal, V.A., Mudaliar, G.V., Shah, N.K. (2013) Impedance spectroscopic study of corrosion inhibition of Al-Pure by organic Schiff base in hydrochloric acid. Journal of Saudi Chemical Society, **17:** 53-59.

[20] Musa, A.Y., Kadhum, A.A.H., Mohamad, A.B., Takriff, M.S., Chee, E.P. (2012) Inhibition of aluminum corrosion by phthalazinone and synergistic effect of halide ion in 1.0M HCl. Current Applied Physics, **12**: 325–330.

[21] Sherif, E.M. (2006) Effects of 2-amino-5-(ethylthio)-1,3,4-thiadiazole on copper corrosion as a corrosion inhibitor in 3% NaCl solutions. Journal of Applied Surface Science, **252:** 8615-8623.

[22] Hu, L., Zhang, S., Li, W., Hou, B. (2010) Electrochemical and thermodynamic investigation of diniconazole and triadimefon as corrosion inhibitors for copper in synthetic seawater. Corrosion Science, **52:** 2891–2896.

[23] Zhang, Q.B., Hua, Y.X. (2009) Corrosion inhibition of mild steel by alkylimidazolium ionic liquids in hydrochloric acid**.** Electrochimica Acta, **54**: 1881-1887..

[24] Yan, Y., Li, W., Cai, L., Hou, B. (2008) Electrochemical and quantum chemical study of purines as corrosion inhibitors for mild steel in 1M HCl solution**.** Electrochimica Acta, **53**: 5953–5960.

[25] Vazquez, M.V., de Sachez, S.R., Calvoy, E.J., Schiffrin, D.J. (1994) The electrochemical reduction of oxygen on polycrystalline copper in borax buffer. Journal of Electroanalytical Chemistry, **374**: 189–197.

[26] Cere, S., Vazquez, M., de Sanchez, S.R., Schiffrin, D.J. (2001) Surface redox catalysis and reduction kinetics of oxygen on copper–nickel alloys. Journal of Electroanalytical Chemistry, **505:** 118–124.

[27] Metikoˇs -Hukovic, M., ˇSkugor, I., Grubaˇc, Z., Babic, R. (2010) Complexities of corrosion behaviour of copper–nickel alloys under liquid impingement conditions in saline water**.** Electrochimica Acta, **55:** 3123–3129.

[28] Procaccini, R., Schiffrin, D.J. (2009) Oxygen reduction on Cu-Zn alloys. Journal of Applied Electrochemistry, **39:** 177–184.

[29] Kear, G., Barker, B.D., Stokes, K.R., Walsh, F.C. (2004) Flow influenced electrochemical corrosion of nickel aluminium bronze – Part I. Cathodic polarisation. Journal of Applied Electrochemistry **34**: 1235-1240. And Flow influenced electrochemical corrosion of nickel aluminium bronze – Part II. Anodic polarisation and derivation of the mixed potential. Journal of Applied Electrochemistry **34:** 1241-1248.

[30] Sury, P., Otswald, H.R. (1972) On the corrosion behaviour of individual phases present in aluminium bronzes. Corrosion Science, **12:** 77–80.

[31] Chen, B., Liang, C., Fu, D., Ren, D. (2005) Corrosion behavior of Cu and the Cu–Zn–Al shape memory alloy in simulated uterine fluid. Contraception, **72**: 221–224.

[32] Hannay, N.B. (1959). Semiconductors, Reinhold Publishing Corporation, New York.

[33] Macdonald, D.D., Ben-Haim, M., Pallix, J. (1989) Segregation of Alloying Elements into Passive Films. Journal of the Electrochemical Society, **136**: 3269-3273.

[34] Milosev, M., Metikoˇs-Hukovic, (1997) The behaviour of Cu-xNi (x = 10 to 40 wt%) alloys in alkaline solutions containing chloride ions. Electrochimica Acta, **42**: 1537.

[35] Sahin, M., Bilgic, S., Yilmaz, H. (2002) The inhibition effects of some cyclic nitrogen compounds on the corrosion of the steel in NaCl mediums. Applied Surface Science, **195**: 1–7.

[36] Bentiss, F., Lebrini, M., Lagrenee, M. (2005) Thermodynamic characterization of metal dissolution and inhibitor adsorption processes in mild steel/2,5-bis(n-thienyl)-1,3,4-

thiadiazoles/hydrochloric acid system. Corrosion Science, **47:** 2915–2931.

[37] Gerengi, H., Bereket, G., (2012) Adsorption and inhibition effect of benzotriazole on brass-118 and brass-MM55 in artificial seawater. Protection of Metals and Physical Chemistry of Surfaces, **48:** 361–366.

[38] Li, W., He, Q., Pei, C., Hou, B., (2007) Experimental and theoretical investigation of the adsorption behaviour of new triazole derivatives as inhibitors for mild steel corrosion in acid media. Electrochimica Acta, **52**: 6386–6394

[39] Scendo, M., (2007) The effect of purine on the corrosion of copper in chloride solutions Corrosion Science, **49:** 373–390.

[40] Li, W., Zhao, X., Liu, F., Hou, B. (2008) Investigation on inhibition behavior of S-triazole–triazole derivatives in acidic solution. Corrosion Science, **50:** 3261–3266.

[41] Donahue, F.M., Nobe, K. (1965) Theory of Organic Corrosion Inhibitors Adsorption and Linear Free Energy Relationships. Journal of the Electrochemical Society, **112**: 886–891.

[42] Yurt, A., Ulutas, S., Dal, H. (2006) Electrochemical and theoretical investigation on the corrosion of aluminium in acidic solution containing some Schiff bases. Applied Surface Science, **253:** 919–925.

[43] Hoar, T.P., Holliday, R.D. (1953) The inhibition by quinolines and thioureas of the acid dissolution of mild steel. Journal of Applied Electrochemistry, **3**: 502-513.

[44] Cremer, E. (1955). Advances in Catalysis, vol. 7, Academic Press, New York, p. 75

[45] Ismail, K.M., Badawy, W.A. (2000) Electrochemical and XPS investigations of cobalt in KOH solutions. Journal of Applied Electrochemistry, **30:** 1303–1311.

[46] Khaled, K.F. (2006) Applied, Experimental and theoretical study for corrosion inhibition of mild steel in hydrochloric acid solution by some new hydrazine carbodithioic acid derivatives. Surface Science, **252:** 4120-4128.

[47] Hladky, K., Calow, L.M., Dawson, J.L. (1980) Corrosion rates from impedance measurements: An introduction. British Corrosion Journal, **15:** 20-25.

[48] Hitzig, J., Titz, J., Juettner, K., Lorenz, W.J., Schmidt, E. (1984) Frequency response analysis of the Ag/Ag+ system: a partially active electrode approach. Electrochimica Acta, **29**: 287-296.

[49] Liao, X.N., Cao, F.H., Zheng, L.Y., Liu, W.J., Chen, A.N., Zhang, J.Q., Cao, C.A. (2011) Corrosion behaviour of copper under chloride-containing thin electrolyte layer. Corrosion Science, **53**: 3289–3298.